Identify the main molecular mechanism of AT_1 non-desensitization*

Xiaoyun Wang[a†], Xiangrong Liu[a], Xiaoqiang Wang[b], Liqing Wu[a], Suli Zhang[c,d], Huirong Liu[c,d†]

[a] *College of Mathematics, Taiyuan University of Technology, Taiyuan, Shanxi 030024, China*

[b] *Department of Scientific computing, Florida State University, Tallahassee, Florida 32306, USA*

[c] *Department of Physiology and Pathophysiology, School of Basic Medical Sciences, Capital Medical University, Beijing, 100069, China*

[d] *Beijing Key Laboratory of Metabolic Disorders Related Cardiovascular Diseases, Capital Medical University, Beijing, 100069, China*

Abstract

Angiotensin II Type 1 Receptor Autoantibodies (AT1-AA) as a functional receptor activator can persistently activate Angiotensin II Type 1 Receptor (AT_1R) by causing AT_1R non-desensitization which is one of the important pathogenesis of preeclampsia (PE). However, the molecular mechanisms of AT1-AA results AT_1R non-desensitization remain unknown. In order to explore the background molecular mechanisms of AT_1R non-desensitization induced by AT1-AA, in this paper we construct dynamical models which are composed of control model (based on the body of healthy pregnant women) and experimental group models (based on the body of pregnant women with preeclampsia). We also consider the effect of membrane fluidity on the reaction when building the dynamical models. In the experiment group models, we established two models that caused AT_1R non-desensitization: endocytosis disorders model and conformation changes model. We wrote C++ and MATLAB programs to do the data fitting. By comparing the data fitting results and analyzing the images of models and corresponding Bayesian information criterion (BIC) values, we conclude that conformation changes may be the key molecular mechanism of AT_1R non-desensitization.

*Project supported by the National Natural Science Foundation of China (91539205, 11801398), the Talent Introduction Research Fund of Taiyuan University of Technology (tyut-rc201317a) and China Scholarship Council. Xiaoqiang Wang's research is partially supported by the US National Science Foundation under grant number DMS-1819059.

† Corresponding author Xiaoyun Wang: xywang0708@126.com and Huirong Liu: Liuhr@126.com.

Keywords: preeclampsia, AT_1R non-desensitization, molecular mechanism.

1 Introduction

Preeclampsia (PE) is a more dangerous type of hypertensive disorder during pregnancy [1]. Pregnant women with normal blood pressure before pregnancy develop hypertension and proteinuria after 20 weeks of gestation. In severe cases, the mother will have cardiopulmonary failure and Hemolysis elevated liver enzymes low platelets (HELLP) syndrome, and a series of complications such as Disseminated Intravascular Coagulation (DIC), fetal intrauterine growth retardation, premature birth, perinatal death, etc. The latest data show that about 30% of premature delivery (less than 32 weeks of gestation) are caused by severe preeclampsia, which is a serious threat to the health of pregnant women and fetuses [2,3].

Studies have shown that the occurrence of PE is related to the three molecules: Ang II (angiotensin II), AT1-AA and AT_1R. AT_1R is abundantly distributed in smooth muscle cells. Under normal conditions, when its physiological ligand Ang II is activated, AT_1R can trigger intracellular signaling, such as Ca^{2+} signal generation and protein kinase C, leading to contraction of vascular smooth muscle cells. In the case of preeclampsia, when AT_1R is over activated by AT1-AA, it causes the blood vessels to continue to contract. The persistent vasoconstriction not only affects the blood vessels of the mother, causes vascular damage and high blood pressure, but also produces a poor intrauterine growth environment, which is unfavorable to fetal development [4,5].

In recent years, many scholars have made a lot of contributions to PE. For example, Zhang [6] pointed that AT1-AA was able to cause amplification response to angiotensin II (Ang II) probably via the calcium-independent protein kinase C pathway, which may provide a new therapy strategy for PE. Zhang [7] demonstrated that AT1-AA mediated heme oxygenase-1 (HO-1) reduction contributes to reduce spiral artery remodeling, and is one main mechanism whereby AT1-AA mediates hypertension and intrauterine growth retardation. In other words, PE is caused by AT_1R non-desensitization. Studies have confirmed that AT_1R non-desensitization (persistent vasoconstriction which is caused by the excessive activation of AT_1R induces abnormal vascular tone and remodeling) is an important pathogenesis of PE.

In the light of current studies, we know that AT1-AA can persistently activate angiotensin

II type-1 receptor (AT_1R), moreover, when the tension of AT1-AA maintains a certain level, it causes AT_1R non-desensitization which may be associated with endocytosis disorders and conformation changes [8].

Before a pregnant woman has preeclampsia, the normal endocytosis is that Ang II in the blood combines to AT_1R, which is widely distributed in the body of pregnant woman, at this time, the cells are activated and the blood pressure is increased. The intermediate complex combined with Ang II and AT_1R is entering the cell, it is decomposed in the cell, and the receptor AT_1R returns to the cell surface and continues to wait for binding to Ang II [9]. Moreover, the cell will return to the inactive state and the blood pressure will decrease, which maintains the balance of blood pressure.

Pregnant women with preeclampsia have AT1-AA in their body, and AT1-AA is a macromolecular protein. When Ang II combines to AT_1R, the blood vessels contract, and the binding products of the two enter the cell, and the blood vessels relax. When the AT1-AA molecule presents extracellularly (that is, the pregnant women have preeclampsia), AT1-AA combines to the receptor AT_1R which could cause vasoconstriction. Because the intermediate complex produced by the combination of AT1-AA and AT_1R is too large, the difficulty of engulfing the cells increases, and the reaction time is lengthened, that is, the time of AT1-AA occupies the receptor AT_1R increases. During this period, normal endocytosis is blocked, which causes the blood vessels to contract for a long time, so that blood pressure rises for a long time [10].

Normally, on the cell membrane, AT_1R is activated after combing of Ang II and AT_1R, the combination product of Ang II and AT_1R enters the cell, then Ang II and AT_1R are separated. At this point, the AT_1R activation process ends and AT_1R circularly proceeds to the previous step. When the combination product of AT1-AA and AT_1R enters the cell, the two are separated, but because the tertiary structure of the protein of AT_1R has changed (protein tertiary structure: the tertiary structure of a protein refers to the relative spatial position of all amino acid residues in the entire peptide chain, that is, the three-dimensional structure of the entire peptide chain), the AT_1R is continuously activated [11]. The AT_1R will be no longer combined with AT1-AA after their separation, resulting in elevated levels of AT1-AA in the blood. This causes the blood vessels to stay at the state of contract for a long time, which will lead to the burst of blood vessels [12].

However, due to the uncertainty of the key molecular mechanism of the AT_1R non-desensitization

[9], we will discuss the possibilities of two molecular mechanisms of AT_1R non-desensitization by establishing the dynamical models.

Based on the above medical phenomenon, we build the relationship diagram of the AT_1R, Ang II and AT1-AA (Figure 1).

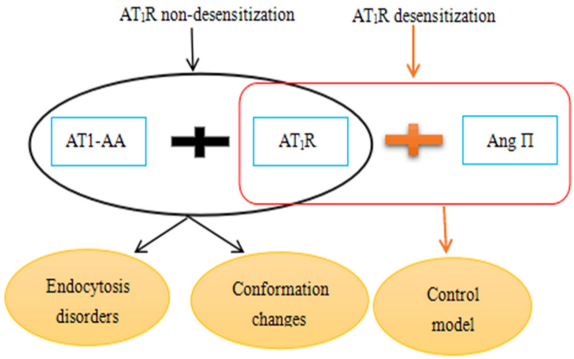

Figure 1 Relationship diagram among the AT_1R, Ang II and AT1-AA.

The Figure 1 shows that AT_1R desensitization is happened when AT_1R and Ang II are combined, which indicates the condition of healthy pregnant women. When pregnant women have preeclampsia, AT_1R and AT1-AA are combined, causing AT_1R non-desensitization. There are two molecular mechanisms that cause AT_1R non-desensitization, namely endocytosis disorders and conformational changes.

This paper is organized as the following. In section 2, we establish the control model (based on the body of healthy pregnant women) and the experimental models (based on the body of pregnant women with preeclampsia): endocytosis disorders model and conformation changes model. Section 3 gives the data sources and data analysis. In section 4, through mathematical calculations and analysis, a series of results were obtained and explained. Section 5 gives the conclusion of this paper.

2 The Establishment of Model

Before establishing the control and experimental models, in order to ensure the rigor of these models, we make some assumptions first:

(A1) The experiments are done in the homogeneous environment.

(A2) The rates of reaction are constant.

(A3) Assuming that the molecular mechanisms of AT_1R non-desensitization are studied, other molecular mechanisms have no effect on it.

2.1 Establishment of a reaction block diagram in the models

Studies have shown that endocytosis disorders and conformational changes are molecular mechanisms that cause AT_1R non-desensitization. In order to clarify which of the two molecular mechanisms is the key molecular mechanism that causes AT_1R non-desensitization, we consider the biological knowledge involved in preeclampsia and establish a complete reaction block diagram with the combination of AT_1R, Ang II and AT1-AA (see Figure 2). By constructing the reaction block diagram, complex biochemical reactions between AT_1R, Ang II and AT1-AA can be transformed into mathematical modeling problems to facilitate the study of preeclampsia symptoms.

On the basis of constructing the reflection block diagram, we regard the combination of AT_1R and Ang II as the control group and the combination of AT_1R and AT1-AA as the experimental group in order to facilitate our research. The control group indicates the condition of healthy pregnant women, and the experimental group indicates the situation of pregnant women with preeclampsia. The reflection block diagram is divided into a control group and an experimental group, to compare the combination of AT_1R, Ang II and AT1-AA in the body of normal pregnant women and pregnant women with preeclampsia. To study the experimental group in more detail, the experimental group was further divided into an endocytosis disorder group and a conformational change group. In this way, we can more clearly understand the difference between the combination of AT_1R and AT1-AA when endocytosis and conformational changes occur separately.

We also used the characteristics of the enzymatic reaction when building the reaction block diagram [13,14]. Enzyme reaction, also known as enzyme catalysis, refers to a chemical reaction catalyzed by an enzyme as a catalyst. Enzymatic reaction is extremely efficient. Enzymes are the most important substances for various chemical reactions in living organisms. The majority of chemical reactions in living organisms are enzymatic reactions [15,16]. The enzyme, like the general catalyst, catalyzes only the thermodynamically permissible chemical reactions (ie, the reverse reaction). Moreover, the enzyme can speed up the chemical reaction without changing the equilibrium point and the equilibrium constant of the reaction.

Finally, by reflecting the establishment of the block diagram, we obtained the normal differential equations of the control group and the experimental group (endocytosis disorders and conformational changes), namely the control group model, endocytosis disorders model and conformational changes model. Among them, the differential equations of each model are provided in the appendix.

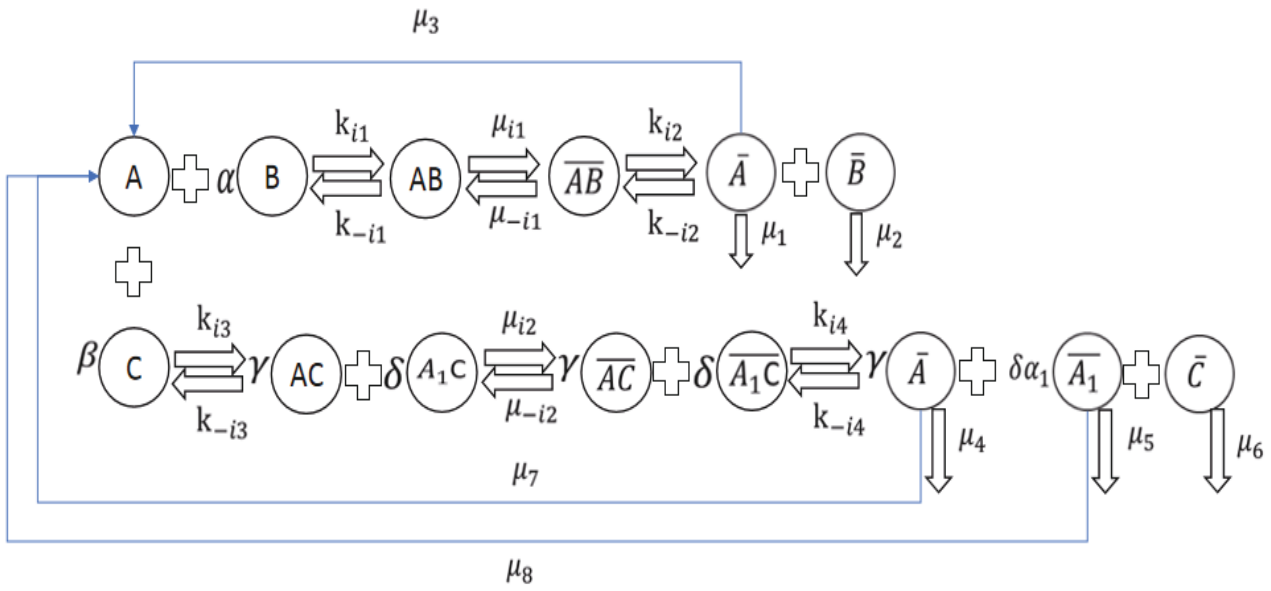

Figure 2 Relation diagram among the AT_1R, Ang II and AT1-AA.

In Figure 2, $i = 1, 2, 3$ (i is the subscript in the reaction rate) indicates the control model, the endocytosis disorders model and the conformational changes model, respectively. Next, we will first give the definition of the value of α, β, γ, δ:

$$\alpha = \begin{cases} 1, & AT_1R \text{ desensitization}, \\ 0, & AT_1R \text{ non-desensitization}, \end{cases} \tag{1}$$

$$\beta = \begin{cases} 1, & AT_1R \text{ non-desensitization}, \\ 0, & AT_1R \text{ desensitization}, \end{cases} \tag{2}$$

$$\gamma = \begin{cases} 1, & AT_1R \text{ non-desensitization by endocytosis disorders}, \\ 0, & AT_1R \text{ non-desensitization by conformational changes}, \end{cases} \tag{3}$$

$$\delta = \begin{cases} 1, & \text{AT}_1\text{R non-desensitization by conformational changes,} \\ 0, & \text{AT}_1\text{R non-desensitization by endocytosis disorders.} \end{cases} \tag{4}$$

In summary:

When $\alpha = 1$, $\beta = 0$, AT_1R is desensitized, which means the situation of healthy pregnant women;

When $\alpha = 0$, $\beta = 1$, AT_1R is not desensitized, which means that the situation of pregnant women with preeclampsia:

(i)when consider AT_1R non-desensitization by endocytosis disorders, $\gamma = 1$, $\delta = 0$.

(ii)when consider AT_1R non-desensitization by conformational changes, $\gamma = 0$, $\delta = 1$.

2.2 Definition of reaction parameters in the model

Several parameters appear in the constructed reaction block diagram. The concentration range of AT_1R, Ang II and AT1-AA is $10^{-8}mol/L \sim 10^{-5}mol/L$, the range of α_1 is $0 \sim 1$. In the following table, we will give the definition of each parameter. (See Table 1, $i = 1, 2, 3$ (i is the subscript in the reaction rate) indicates the control model, the endocytosis disorders model and the conformational changes model, respectively.)

3 Data

3.1 Data Sources

The data are collected in a rat thoracic aorta rings experiments of Capital Medical University in Beijing, China. The preparation of rat thoracic aorta rings: Male Wistar rats weighing 200-250g were anesthetized by injection of 10% chloral hydrate (300mg/kg, i.p.). The thoracic aorta was isolated immediately and placed in ice-cold HEPES physiological buffer (mM) ($NaCl$ 118.2, KCl 4.7, $CaCl$ 2.2, H_2O 2.5, KH_2PO_4 1.2, $MgCl_2$ 1.2, glucose 11.7, $NaHCO_3$ 25.0, and $EDTA$ 0.026) and cut in to rings of about 3-5mm in width and mounted in organ baths containing 2.5mL of normal HEPES solution according to the method developed by Nicosia [15] et al originally in 1990 with minor modifications. The bath solution was maintained at 37^{o}C and pH 7.4 by gassing continuously with a mixture of 95% O_2 and 5% CO_2. After

Table 1: Definitions of the parameters used in three models

Parameters	Definition	Value	References
$[A_0]$	Initial concentration value of AT_1R (mol/L)	5×10^{-6}	[a]
$[B_0]$	Initial concentration value of Ang II (mol/L)	2×10^{-6}	[a]
$[C_0]$	Initial concentration value of AT1-AA (mol/L)	2×10^{-6}	[a]
k_{i1}, k_{i3}	Positive reaction rate in models $(M^{-1}min^{-1})$		estimated
k_{-i1}, k_{-i3}	Reverse reaction rate in models (min^{-1})		estimated
k_{i2}, k_{i4}	Positive reaction rate in models (min^{-1})		estimated
k_{-i2}, k_{-i4}	Reverse reaction rate in models (min^{-1})		estimated
μ_{i1}, μ_{i2}	Rate of entering cells in models (min^{-1})		estimated
μ_{-i1}, μ_{-i2}	Rate of transfer to the outside of the cell (min^{-1})		estimated
μ_1, μ_2	Degradation rate in control model (min^{-1})		estimated
μ_4, μ_5, μ_6	Degradation rate in experiment models (min^{-1})		estimated
μ_3	Rate of return to the cell surface (min^{-1})		estimated
μ_7, μ_8	Rate of return to the cell surface (min^{-1})		estimated
α_1	The ratio of molecular mechanism		estimated

[a] Beijing Key Laboratory of Metabolic Disorders Related Cardiovascular Diseases, Capital Medical University, Beijing.

equilibration for 60 min at the optimal resting tension of $2g$, aortic rings were subjected with KCl (mM) to assure the ideal contractile condition of the preparation. And then specific experimental protocols were initiated. The contractile response was measured via a force-displacement transducer (DMT610M, Danish Myo Technology) coupled with a data recording system. Based on a large number of the rat thoracic aorta rings experiments, we get the data of medical experiments. The study conformed to AVMA Guidelines on Euthanasia and the Guide for the Care and Use of Laboratory Animals protocol published by the Ministry of the People Republic of China. All studies were approved by Capital Medical University Committee on Animal Care.

3.2 Data Analysis

Considering the influence of temperature and other factors on the experimental data, the precise range of error is given in the data. Through the experimental measurement, we obtained the contraction response data of the rat thoracic aorta rings in the control group and the experimental group respectively (see Table 2 and Table 3), and obtained the images of the trend of the size of the contraction response data in the control group and the experimental group by using MATLAB (see Figure 3). Wherein, the abscissa in the image represents the time, and the ordinate represents the size of the contraction reaction data at the time point, and the unit is mN.

However, when we use mathematical model to analyze and calculate, the established differential equation system generally indicates the relationship between concentration and time, but the data obtained from the experiment is the relationship between the contraction response data size and time. Therefore, we need to transform the relationship between the contraction response data size and time into the relationship between concentration and time. Jochen Steppan [16] pointed out that when the vasopressin concentrations in the range of $10^{-8}mol/L \sim 10^{-5}mol/L$, the cell tension and vasopressin concentrations can be seen as a directly proportional relationship. That is, there is a linear relationship between the shrinkage reaction and the concentration, and the scale factor is assumed to be a, which is determined by our C++ program during the data fitting.

Table 2 and Table 3 are the time-dependent data of the contractile response in control model and experiment models (endocytosis disorders model, conformation changes model),

Table 2: The contractile response data in control model

Time (min)	Initial values (mN)	Values range (mN)	Time (min)	Initial values (mN)	Values range (mN)
0	0	0	2.25	1.65	1.65 ± 0.01
0.18	0.15	0.15 ± 0.01	2.50	1.55	1.55 ± 0.01
0.33	0.29	0.29 ± 0.01	2.67	1.22	1.22 ± 0.01
0.50	0.68	0.68 ± 0.01	2.92	1.00	1.00 ± 0.01
0.67	1.15	1.15 ± 0.01	3.33	0.78	0.78 ± 0.01
0.75	1.65	1.65 ± 0.01	3.67	0.64	0.64 ± 0.01
0.83	2.00	2.00 ± 0.01	3.83	0.42	0.42 ± 0.01
1.17	2.20	2.20 ± 0.01	4.17	0.35	0.35 ± 0.01
1.42	2.36	2.36 ± 0.01	4.50	0.31	0.31 ± 0.01
1.67	2.26	2.26 ± 0.01	4.67	0.29	0.29 ± 0.01
2.00	2.00	2.00 ± 0.01	5.00	0.23	0.23 ± 0.01

respectively. Figure 2(a) and Figure 2(b) are the corresponding table 2 and table 3 of the graph, respectively.

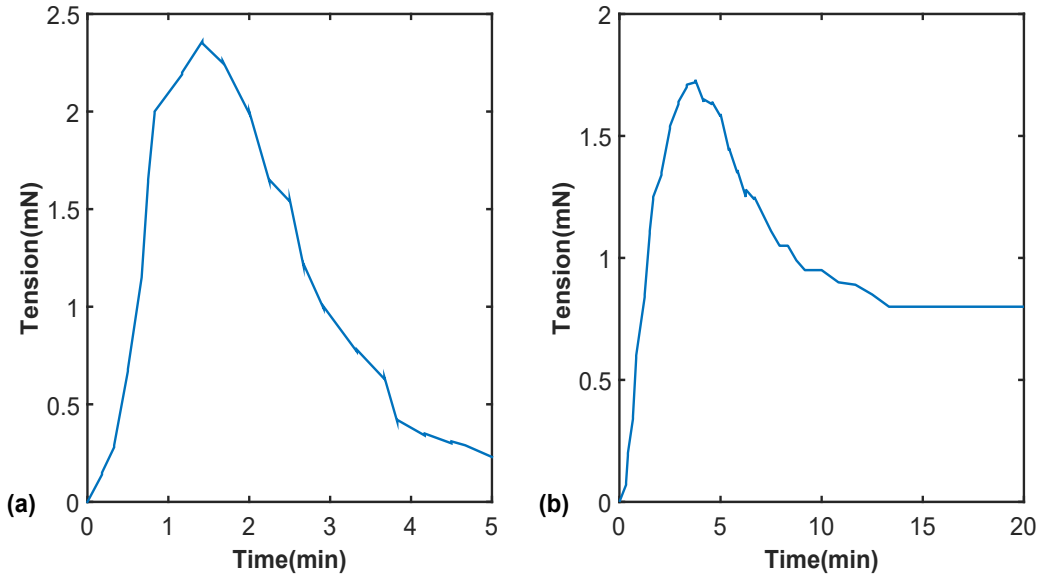

Figure 3 The images of the contractile response data. **(a)** Data of medical experiments in control model. **(b)** Data of medical experiments in experiment models.

Figure 3 represents that the trend of thoracic aorta contractile response in rats with time. Figure 3(a) reflects that the effect of angiotensin II receptor-1 (AT1-AA) on the contractile

Table 3: The contractile response data in experiment models

Time (min)	Initial values (mN)	Values range (mN)	Time (min)	Initial values (mN)	Values range (mN)
0	0	0			
0.33	0.15	0.08 ± 0.01	7.50	1.55	1.11 ± 0.01
0.42	0.29	0.20 ± 0.01	7.92	1.22	1.05 ± 0.01
0.67	0.68	0.35 ± 0.01	8.33	1.00	1.05 ± 0.01
0.83	1.15	0.60 ± 0.01	8.75	0.78	0.99 ± 0.01
1.25	1.65	0.85 ± 0.01	9.17	0.64	0.95 ± 0.01
1.50	2.00	1.11 ± 0.01	9.58	0.42	0.95 ± 0.01
1.67	2.20	1.25 ± 0.01	10.00	0.35	0.95 ± 0.01
2.08	2.36	1.35 ± 0.01	10.83	0.31	0.90 ± 0.01
2.50	2.26	1.54 ± 0.01	11.67	0.29	0.89 ± 0.01
2.92	2.00	1.64 ± 0.01	12.50	0.23	0.85 ± 0.01
3.33	0.29	1.71 ± 0.01	13.33	1.22	0.80 ± 0.01
3.75	0.68	1.73 ± 0.01	14.17	1.00	0.80 ± 0.01
4.17	1.15	1.65 ± 0.01	15.00	0.78	0.80 ± 0.01
4.58	1.65	1.64 ± 0.01	15.83	0.64	0.80 ± 0.01
5.00	2.00	1.59 ± 0.01	16.67	0.42	0.80 ± 0.01
5.42	2.20	1.45 ± 0.01	17.50	0.35	0.80 ± 0.01
5.83	2.36	1.36 ± 0.01	18.83	0.31	0.80 ± 0.01
6.25	2.26	1.27 ± 0.01	19.17	0.29	0.80 ± 0.01
6.67	2.00	1.25 ± 0.01	20.00	0.23	0.80 ± 0.01

response of rat thoracic aorta. Figure 3(b) shows that the effect of Autoantibody against angiotensin II receptor-1 (AT1-AA) on the contractile response of rat thoracic aorta.

4 Results

In the experimental group models, the combination of AT1-AA and AT_1R forms a complex, then the complex transforms into an intracellular composite product at a certain rate. The change of the concentration of the intracellular composite product is selected to fit the image because it is related to the measurement of the contractile response data. The reason why the concentration trend of the intracellular composite product is selected in the control model to fit the image is also the same.

We wrote a C++ program to do the data fitting. It mainly uses least squares method and maximum likelihood estimation to find the optimal values of the unknown parameters listed in Table 1, as well as the scale parameter a between the shrinkage reaction and the concentration. After all the parameters were determined, we put them back to the differential equations. By using 2nd order Runge-Kutta method, we can solve the differential equation system. And the results, i.e., the concentration graphs of intracellular composite products of models are plotted by a MATLAB program. We did the data fitting for all the three models: control model, endocytosis disorders model and the conformation changes model. Table 4 lists the rate values obtained by the procedures of these three models, where $i = 1, 2, 3$, indicating the control model, the endocytosis disorders model and the conformational changes model, respectively.

Note: " $-$ " indicates that it is not discussed in this range.

4.1 Analysis of the obtained reaction parameters

From Table 4, we can get:

(1) In control model: the positive reaction rate (k_{11}) of the control group model is smaller than the corresponding positive reaction rate (k_{23} and k_{33}) of the endocytosis disorders model and the conformation changes model. However, the rate (μ_{11}) at which the complex (AB) of the control model entered the cell was much greater than the rate (μ_{22}) at which the complex (AC) of the endocytosis disorders model entered the cell and the rate (μ_{32}) at which the complex (A_1C) of the conformation changes model entered the cell. Therefore, the complex (AB) of the

Table 4: Rate values in three models

Case	control model	endocytosis disorders model	conformation changes model
k_{i1} $(M^{-1}min^{-1})$	0.807518	-	-
k_{-i1} (min^{-1})	0.095631	-	-
μ_{i1} (min^{-1})	1.502718	-	-
μ_{-i1} (min^{-1})	0.178332	-	-
k_{i2} (min^{-1})	0.619688	-	-
k_{-i2} (min^{-1})	0.071522	-	-
k_{i3} $(M^{-1}min^{-1})$	-	1.035346	1.018103
k_{-i3} (min^{-1})	-	0.000743	0.699654
μ_{i2} (min^{-1})	-	0.425618	0.586959
μ_{-i2} (min^{-1})	-	0.135341	0.402726
k_{i4} (min^{-1})	-	0.278210	0.179400
k_{-i4} (min^{-1})	-	0.089525	0.097684
μ_1 (min^{-1})	0.102415	-	-
μ_2 (min^{-1})	0.100667	-	-
μ_3 (min^{-1})	0.798414	-	-
μ_4 (min^{-1})	-	0.000363	-
μ_5 (min^{-1})	-	-	0.001139
μ_6 (min^{-1})	-	0.000362	0.000362
μ_7 (min^{-1})	-	0.000362	-
μ_8 (min^{-1})	-	-	0.893137
α_1	-	-	0.001742
BIC	-	-212.7512	-236.7354

control model rapidly enters the cell and is converted into an intracellular complex ($\overline{AB}$), then the intracellular complex ($\overline{AB}$) is decomposed into the final product ($\overline{A}$ and $\overline{B}$) at the rate of k_{12}, and its rate of decomposition (k_{12}) is greater than the corresponding rate of decomposition (k_{24} and k_{34}) in the endocytosis disorders model and the conformation changes model. In addition, the control products ($\overline{A}$ and $\overline{B}$) were apoptotic at almost the same rate of degradation (μ_1 and μ_2), and the product ($\overline{A}$) was returned to the cell surface at a rate μ_3 which is greater than its rate of degradation (μ_1) to reduce to AT_1R.

(2) In endocytosis disorders model: the positive reaction rate (k_{23}) of the endocytosis disorders model is greater than the positive reaction rate (k_{11}) in the control model and the positive reaction rate (k_{33}) in the conformation changes model, indicating that the combination of AT_1R and AT1-AA rapidly generates complex (AC). The reverse reaction rate (k_{-23}) in the model is almost equal to 0, which is much smaller than the reverse reaction rate (k_{-11}) in the control model and the reverse reaction rate (k_{-33}) in the conformation changes model, which means that the complex (AC) formed by the combination of AT_1R and AT1-AA is difficult to convert to AT_1R and AT1-AA. However, the rate (μ_{22}) at which the complex (AC) enters the cell into an intracellular complex ($\overline{AC}$) is much less than the rate (μ_{11}) at which the complex (AB) of the control model enters the cell into an intracellular complex ($\overline{AB}$), further indicating that AT1-AA is macromolecular protein, when it combined with AT_1R, AT1-AA has barriers to entry into the cell, that is, it is difficult to enter the cell. At the same time, the complex (AC) enters the cell and transform into an intracellular complex ($\overline{AC}$), and $\overline{AC}$ is decomposed into the final product ($\overline{A}$ and $\overline{C}$) at the decomposition rate k_{24}, and its decomposition rate (k_{24}) is smaller than that of the intracellular complex ($\overline{AB}$) in the control model (k_{12}). In addition, the final product ($\overline{A}$ and $\overline{C}$) of the endocytosis disorders model was apoptotic at a degradation rate (μ_4 and μ_6) close to zero, respectively, and the product ($\overline{A}$) was returned to the cell surface at the same small transfer rate (μ_7) to reduce to AT_1R.

(3) In conformation changes model: the positive reaction rate (k_{33}) of the conformation changes model is greater than the positive reaction rate (k_{11}) in the control model and less than the positive reaction rate (k_{23}) in the endocytosis disorders model. The rate of reverse reaction (k_{-33}) in the model is much higher than the rate of reverse reaction (k_{-11}) in the control model and the rate of reverse reaction (k_{-23}) in the endocytosis disorders model, ie the complex (A_1C) formed by the combination of AT_1R and AT1-AA is decomposed into AT_1R and AT1-AA

at a faster decomposition rate. This is because the structure of AT_1R has changed when the conformational change occurs, the concentration of AT_1R is abnormally lowered, and AT1-AA continuously activates AT_1R, so the complex (A_1C) formed by the combination of AT_1R and AT1-AA is quickly decompose into AT_1R and AT1-AA. At the same time, the rate (μ_{32}) at which the complex (A_1C) enters the cell into an intracellular complex $(\overline{A_1C})$ is greater than the rate (μ_{22}) at which the complex (AC) enters the cell into an intracellular complex $(\overline{AC})$ in the endocytosis disorders model. Moreover, the intracellular complex $(\overline{A_1C})$ is decomposed into a final product $(\overline{A_1}$ and $\overline{C})$ at a rate of decomposition (k_{34}), which is less than the rate of decomposition (k_{24}) of the intracellular complex $(\overline{AC})$ into the final product $(\overline{A}$ and $\overline{C})$ in the endocytosis disorders model. At the same time, the final product $(\overline{A_1}$ and $\overline{C})$ is apoptotic at a rate of degradation $(\mu_5$ and $\mu_6)$, and the product $(\overline{A_1})$ is returned to the cell surface at a metastatic rate (μ_8) to reduce to AT_1R. Among them, the metastasis rate (μ_8) is much greater than the rate of metastasis (μ_7) of the product of the endocytosis disorders model $(\overline{A})$ returned to the cell surface and converted to AT_1R.

4.2 Analysis of the obtained graphs

Substituting the optional rate values of the Table 4 into the three models respectively, the concentration graphs of intracellular complex of three models could be gained. The Figure 4 lists the images of three models (including control model, endocytosis disorders model and conformation changes model).

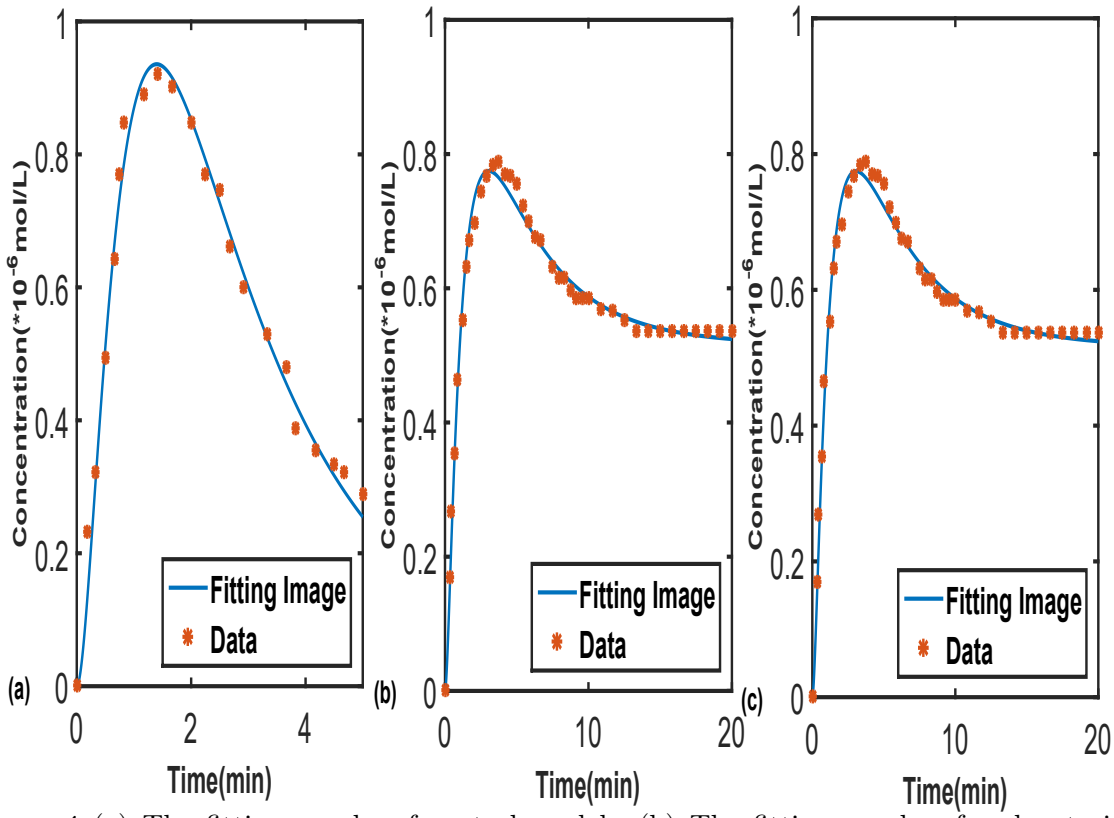

Figure 4 (a) The fitting graphs of control model. (b) The fitting graphs of endocytosis disorder model. (c) The fitting graphs of conformational change model.

Figure 4(a) shows that the fitting result of control model from 0 to 5 min, where the dots are twenty-two measured values and this curve is the trend of the concentration of intracellular complex $\overline{AB}$ in control model. From the concentration of $\overline{AB}$ image, we can see that the concentration of $\overline{AB}$ rises rapidly until it reaches a maximum value at about 1.42 min, then falls rapidly from 1.42 to 5 min, which shows that Ang II and AT_1R react normally, causing AT_1R desensitization in healthy pregnant women.

Figure 4(b) expresses that the fitting result of endocytosis disorders model from 0 to 20 min, where the dots are thirteen-nine measured values and this curve is the trend of the concentration of intracellular complex $\overline{AC}$ in endocytosis disorders model. Based on the concentration of $\overline{AC}$ image, we can notice that the concentration of $\overline{AC}$ rises rapidly until it reaches a maximum value at about 3.75 min and falls from 3.75 to 12 min, hereafter it tends to stable.

Figure 4(c) represents that the fitting result of conformation changes model from 0 to 20 min, where the curve is the trend of the concentration of intracellular complex $\overline{A_1C}$ in conformation changes model. According to the concentration of $\overline{A_1C}$ image, we can note that

the concentration of $\overline{A_1C}$ rises rapidly until it reaches a maximum value at about 3.75 min and falls from 3.75 to 15.5 min, subsequently, it tends to steady.

4.3 Analysis of the obtained predictive models

We apply the above obtained parameters and forecast the images of the concentration of intracellular complex of three models which including control model, endocytosis disorders model and conformation changes model between 100 min. we can give the following images:

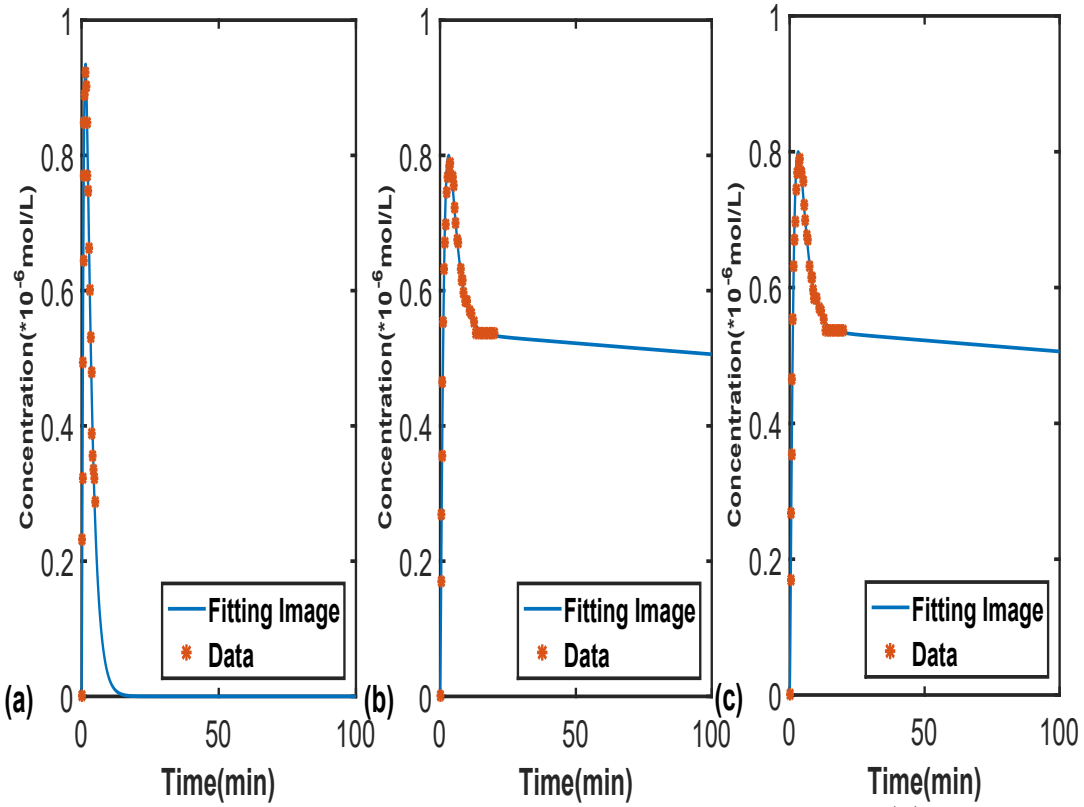

Figure 5 The fitting and prediction graphs of control model at 120 min. (b) The fitting and prediction graphs of endocytosis disorder model at 120 min. (c) The fitting and prediction graphs of conformational change model at 120 min.

Figure 5(a) shows that the prediction result of control model from 0 to 120 min, the concentration of intracellular complex $\overline{AB}$ rises rapidly to the maximum and then continues to decrease, until the value is 0 at about 15 min, subsequently, the value of the concentration remains at 0.

Figure 5(b) indicates that the prediction result of endocytosis disorder model from 0 to 120 min, the concentration of intracellular complex $\overline{AC}$ rises rapidly to the maximum and then

continues to drop, finally the value keeps steady from 12 to 120 min.

Figure 5(c) represents that the prediction result of conformational changes model from 0 to 120 min, the concentration of intracellular complex $\overline{A_1C}$ also rapidly rise to the maximum and then continues to decline, then the value keeps stable from 15.5 to 120 min.

5 Conclusion

From Figure 4 and Figure 5, we can get:

(1) The time of the concentration of intracellular complex $\overline{AB}$ reaches the maximum value in control model faster than the experimental models (endocytosis disorder model and conformation changes model). In addition, the maximum of the concentration of $\overline{AB}$ in control model is a bit larger than the maximum of the concentration of intracellular complex $\overline{AC}$ of the endocytosis disorder model and the maximum of the concentration of intracellular complex $\overline{A_1C}$ of the conformation changes model.

(2) The concentration of intracellular complex $\overline{AB}$ has been 0 since about 15 min in control model, and the concentration of intracellular complex $\overline{AC}$ is steady from about 12 minutes, the concentration of intracellular complex $\overline{A_1C}$ is stable from about 15.5 minutes. We can easily note that AT1-AA (C) could affect the normal reaction of AT_1R (A) and Ang II (B) in the body of pregnant woman, leading to the intracellular complex does not break down completely in short time, which may be the major reason of AT_1R non-desensitization.

In this paper, by analyzing the parameters and images of the models of the main molecular mechanisms causing AT_1R non-desensitization, BIC values corresponding to two results in endocytosis disorder model and conformation changes model are -212.7512, -236.7354, respectively. We can easily notice that $BIC_2 < BIC_1$, $BIC_{min} = BIC_2 = -236.7354$. Based on Bayesian information criterion (the smaller the BIC value, the better), it is judged from the calculated BIC values that the conformation changes model is the best, that is, conformational change may be the main major molecular mechanisms of AT_1R non-desensitization, and the endocytosis disorders may have slight affect.

A Differential equation of the control model

First, we consider the control model based on Figure 2 with regard to normal pregnant women. The time evolution of control model is described by six coupled differential equations:

$$\begin{cases} \frac{\mathrm{d}[A]}{\mathrm{d}t} &= -k_{11}[A][B] + k_{-11}[AB] + \mu_3[\overline{A}], \\ \frac{\mathrm{d}[B]}{\mathrm{d}t} &= -k_{11}[A][B] + k_{-11}[AB], \\ \frac{\mathrm{d}[AB]}{\mathrm{d}t} &= k_{11}[A][B] - k_{-11}[AB] - \mu_{11}[AB] + \mu_{-11}[\overline{AB}], \\ \frac{\mathrm{d}[\overline{AB}]}{\mathrm{d}t} &= \mu_{11}[AB] - \mu_{-11}[\overline{AB}] - k_{12}[\overline{AB}] + k_{-12}[\overline{A}][\overline{B}], \\ \frac{\mathrm{d}[\overline{A}]}{\mathrm{d}t} &= k_{12}[\overline{AB}] - k_{-12}[\overline{A}][\overline{B}] - \mu_1[\overline{A}] - \mu_3[\overline{A}], \\ \frac{\mathrm{d}[\overline{B}]}{\mathrm{d}t} &= k_{12}[\overline{AB}] - k_{-12}[\overline{A}][\overline{B}] - \mu_2[\overline{B}], \end{cases} \tag{5}$$

where the initial conditions of the control model are $[A](0) = [A_0] = 5 \times 10^{-6} mol/L$, $[B](0) = [B_0] = 2 \times 10^{-6} mol/L$, $[AB](0) = 0$, $[\overline{AB}](0) = 0$, $[\overline{A}](0) = 0$, $[\overline{B}](0) = 0$.

B Differential equation of the endocytosis disorders model

We know that AT1-AA could specifically recognize the second extracellular loop of AT_1R (AT_1R-ECII) [4]. So AT1-AA and Ang II compete for different binding sites of AT_1R, which belong to the competitive inhibition in different positions of AT_1R [17]. When AT1-AA wants to enter the cell to react with AT_1R, while AT1-AA fails to enter the cell, which leads to the occurrence of endocytosis disorders. The time evolution of endocytosis disorders model that base on Figure 2 is described by six coupled differential equations :

$$\begin{cases} \frac{\mathrm{d}[A]}{\mathrm{d}t} &= -k_{23}[A][C] + k_{-23}[AC] + \mu_7[\overline{A}], \\ \frac{\mathrm{d}[C]}{\mathrm{d}t} &= -k_{23}[A][C] + k_{-23}[AC], \\ \frac{\mathrm{d}[AC]}{\mathrm{d}t} &= k_{23}[A][C] - k_{-23}[AC] - \mu_{22}[AC] + \mu_{-22}[\overline{AC}], \\ \frac{\mathrm{d}[\overline{AC}]}{\mathrm{d}t} &= \mu_{22}[AC] - \mu_{-22}[\overline{AC}] - k_{24}[\overline{AC}] + k_{-24}[\overline{A}][\overline{C}], \\ \frac{\mathrm{d}[\overline{A}]}{\mathrm{d}t} &= k_{24}[\overline{AC}] - k_{-24}[\overline{A}][\overline{C}] - \mu_4[\overline{A}] - \mu_7[\overline{A}], \\ \frac{\mathrm{d}[\overline{C}]}{\mathrm{d}t} &= k_{24}[\overline{AC}] - k_{-24}[\overline{A}][\overline{C}] - \mu_6[\overline{C}], \end{cases} \tag{6}$$

where the initial conditions of the endocytosis disorders model are $[A](0) = [A_0] = 5 \times 10^{-6} mol/L$, $[B](0) = [B_0] = 2 \times 10^{-6} mol/L$, $[AC](0) = 0$, $[\overline{AC}](0) = 0$, $[\overline{A}](0) = 0$, $[\overline{C}](0) = 0$.

C Differential equation of the conformation changes model

When AT1-AA reacted with AT_1R, the structure of AT_1R has changed. The coupled differential equations for the conformation changes model which based on Figure 2 can be built as :

$$\begin{cases} \frac{\mathrm{d}[A]}{\mathrm{d}t} &= -k_{33}[A][C] + k_{-33}[A_1C] + \mu_8[\overline{A}]^{\alpha_1}, \\ \frac{\mathrm{d}[C]}{\mathrm{d}t} &= -k_{33}[A][C] + k_{-33}[A_1C], \\ \frac{\mathrm{d}[A_1C]}{\mathrm{d}t} &= k_{33}[A][C] - k_{-33}[A_1C] - \mu_{32}[A_1C] + \mu_{-32}[\overline{A_1C}], \\ \frac{\mathrm{d}[\overline{A_1C}]}{\mathrm{d}t} &= \mu_{32}[A_1C] - \mu_{-32}[\overline{A_1C}] - k_{24}[\overline{A_1C}] + k_{-24}[\overline{A}]^{\alpha_1}[\overline{C}], \\ \frac{\mathrm{d}[\overline{A}]}{\mathrm{d}t} &= \alpha_1 \times k_{24}[\overline{A_1C}] - \alpha_1 \times k_{-24}[\overline{A}]^{\alpha_1}[\overline{C}] - \alpha_1 \times \mu_5[\overline{A}]^{\alpha_1} - \alpha_1 \times \mu_8[\overline{A}]^{\alpha_1}, \\ \frac{\mathrm{d}[\overline{C}]}{\mathrm{d}t} &= k_{24}[\overline{AC}] - k_{-24}[\overline{A}]^{\alpha_1}[\overline{C}] - \mu_6[\overline{C}], \end{cases} \tag{7}$$

where the initial conditions of the conformation changes model are $[A](0) = [A_0] = 5 \times 10^{-6} mol/L$, $[B](0) = [B_0] = 2 \times 10^{-6} mol/L$, $[A_1C](0) = 0$, $[\overline{A_1C}](0) = 0$, $[\overline{A_1}](0) = 0$, $[\overline{C}](0) = 0$.

D Select the optimal model with BIC

Next, we will select the optimal model by the application of BIC to determine a possible major molecular mechanism of the AT_1R non-desensitization.

We make use of Bayesian information criterion (BIC) to seek a model fit to the actual data best. The Bayesian information criterion is defined as follows:

$$BIC = N_z \ln \hat{\sigma}^2 + P_k \ln N_z, N_k = P_k + 1,$$

where $\hat{\sigma}^2$ is an Maximum likelihood (ML) estimate, N_z is the number of the real data and P_k is the total amount of estimated parameters in the model. Since control model is a model in

a normal human body, we only need to calculate the BIC values of the experimental models (endocytosis disorder model and conformation changes model).

The BIC of endocytosis disorders model:

$$\hat{\sigma}_1^2 = 0.00183521,$$

$$BIC_1 = 39 \ln \hat{\sigma}_1^2 + 9 \ln 39 = -212.7512.$$

The BIC of conformation changes model:

$$\hat{\sigma}_2^2 = 0.00099221,$$

$$BIC_2 = 39 \ln \hat{\sigma}_2^2 + 9 \ln 39 = -236.7354.$$

References

[1] Ranjkesh, F., Jaliseh, H.K., Abutorabi, S. Monitoring the copper content of serum and urine in pregnancies complicated by preeclampsia. Biol Trace Elem Res. 144, 58-62(2011).

[2] Herse, F., LaMarca, B. Angiotensin II Type 1 Receptor Autoantibody (AT1-AA) - Mediated Pregnancy Hypertension. Am J Reprod Immunol. 69, 413(2013).

[3] Baumwell, S., Karumanchi, S.A. Pre-eclampsia: clinical manifestations and molecular mechanisms. Nephron Clin Pract. 2, 72-81(2007).

[4] Wallukat, G., Homuth, V. et al. Patients with preeclampsia develop agonistic autoantibodies against the angiotensin AT1 receptor. J. Clin. Invest. 103, 945-952(1999).

[5] Ye, Y. et al. Complement Split Products C3a/C5a and Receptors: Are They Regulated by Circulating Angiotensin II Type 1 Receptor Autoantibody in Severe Preeclampsia? Gynecol Obstet Inves. 81, 28-33(2016).

[6] Zhang, W. et al. Mechanism of agonistic angiotensin II type 1 receptor autoantibody-amplified contractile response to AngII in the isolated rat thoracic aorta. Acta Bioch Biop Sin. 47, 851-856(2015).

[7] Zhang, D. et al. The Role of the Reduction of Spiral Artery Remodeling and Heme Oxygenase 1 in Mediating AT1-AA-Induced Hypertension and Intrauterine Growth Restriction in Pregnant Rats. Am J Perinat. 31, 883-90(2014).

[8] Bornholz, B. et al. Impact of human autoantibodies on β 1-adrenergic receptor conformation, activity, and internalization. Cardiovasc Res. 97, 472-480(2013).

[9] Baumwell, S., Karumanchi, S.A. Pre-eclampsia: clinical manifestations and molecular mechanisms. Nephron Clin Pract. 2, 72-81(2007).

[10] Hunyady, L. et al. Differential PI 3-kinase dependence of early and late phases of recycling of the internalized AT1 angiotensin receptor. J Cell Biol. 157, 1211-1222(2002).

[11] Zhang, S.L. et al. Angiotensin type 1 receptor autoantibody from preeclamptic patients induces human fetoplacental vasoconstriction. J Cell Physiol. 228, 142-148(2013).

[12] Ekmekci, O. B., Ekmekci, H. et al. Evaluation of Lp-PLA2 mass, vitronectin and PAI-1 activity levels in patients with preeclampsia. Arch Gynecol Obstet. 292, 53-58(2015).

[13] Thway, T. M., Shlykov, S. G. et al. Antibodies from preeclamptic patients stimulate increased intracellular Ca2+ mobilization through angiotensin receptor activation. Circulation. 110, 1612-1619(2004).

[14] Yang, F. et al. Autoantibody against AT1 receptor from preeclamptic patients induces vasoconstriction through angiotensin receptor activation. J Hypertens. 26, 1629-1635(2008).

[15] Nicosia, R.F., Ottinetti, A. Growth of microvessels in serum-free matrix culture of rat aorta. Lab Invest. 63, 115-22(1990).

[16] Jochen, S., et al. Vasopression-Mediated enhancement of adrenergic vasoconstriction involves both the tyrosine kinase and the protein kinase C pathways. ISAP. 115: 1290-1295(2012).

[17] Lohith, K., Manohar, B., Divakar, S. Competitive inhibition by substrates of the esterification reaction between l-phenylalanine and d-glucose catalysed by the lipases of Rhizomucor miehei and Candida rugosa. World J of Microb and Biot. 23, 955-964(2007).

Contributions

Xiaoyun Wang and Xiangrong Liu built models, processed the data, simulated the images, wrote and modifed the manuscript. Xiaoqiang Wang wrote related C++ programs, helped to analyze the experiments and polished the manuscript. Suli Zhang and Huirong Liu designed and performed the experimentations.

Competing interests

The authors declare no competing financial interests.